AMERICAN SOCIETY FOR MICROBIOLOGY | Molecular and Cellular Biology

GGA3 Interacts with a G Protein-Coupled Receptor and Modulates Its Cell Surface Export

Maoxiang Zhang, Jason E. Davis, Chunman Li, Jie Gao, Wei Huang, Nevin A. Lambert, Alvin V. Terry, Jr., Guangyu Wu

Department of Pharmacology and Toxicology, Medical College of Georgia, Augusta University, Augusta, Georgia, USA

Molecular mechanisms governing the anterograde trafficking of nascent G protein-coupled receptors (GPCRs) are poorly understood. Here, we have studied the regulation of cell surface transport of α_2-adrenergic receptors (α_2-ARs) by GGA3 (Golgi-localized, γ-adaptin ear domain homology, ADP ribosylation factor-binding protein 3), a multidomain clathrin adaptor protein that sorts cargo proteins at the *trans*-Golgi network (TGN) to the endosome/lysosome pathway. By using an inducible system, we demonstrated that GGA3 knockdown significantly inhibited the cell surface expression of newly synthesized α_{2B}-AR without altering overall receptor synthesis and internalization. The receptors were arrested in the TGN. Furthermore, GGA3 knockdown attenuated α_{2B}-AR-mediated signaling, including extracellular signal-regulated kinase 1/2 (ERK1/2) activation and cyclic AMP (cAMP) inhibition. More interestingly, GGA3 physically interacted with α_{2B}-AR, and the interaction sites were identified as the triple Arg motif in the third intracellular loop of the receptor and the acidic motif EDWE in the VHS domain of GGA3. In contrast, α_{2A}-AR did not interact with GGA3 and its cell surface export and signaling were not affected by GGA3 knockdown. These data reveal a novel function of GGA3 in export trafficking of a GPCR that is mediated via a specific interaction with the receptor.

G protein-coupled receptors (GPCRs) are the largest superfamily of cell surface receptors and modulate a variety of cell functions under physiological and pathological conditions (1, 2). The functions of GPCRs are highly regulated by elaborately coordinated intracellular trafficking processes, including anterograde export of newly synthesized receptors to the cell surface, endocytosis of the cell surface receptors into the endosomal compartment in response to ligand activation, recycling of the internalized receptors from endosomes back to the plasma membrane, and transport of receptors to lysosomes for degradation. These trafficking processes determine the numbers of receptors at the cell surface available for binding to ligands and thus dictate the magnitude of ligand-elicited cellular responses. Indeed, it has become increasingly apparent that mistrafficking of GPCRs that leads to the dysfunction of the receptors directly links to the pathogenesis of human diseases, such as nephrogenic diabetes insipidus, retinitis pigmentosa, and male pseudohermaphroditism (3–5). However, compared with well-characterized internalization, recycling, and degradation (6, 7), the molecular mechanisms underlying the cell surface transport of nascent GPCRs from the endoplasmic reticulum (ER) through the Golgi apparatus are relatively less well understood.

The Golgi/*trans*-Golgi network (TGN) compartment is often referred to as the "sorting center" where newly synthesized proteins are sorted to be delivered to their final cellular destinations such as endosomes, lysosomes, and the plasma membrane. Post-Golgi transport can be mediated through clathrin-coated transport vesicles, which are composed of clathrin and various adaptor proteins. Adaptor protein complexes (APs), GGAs (Golgi-associated, γ-adaptin homologous, ARF-interacting proteins), and hepatocyte growth factor receptor substrate (Hrs) are well-known adaptor proteins for clathrin-coated vesicles. There are three GGA isoforms (GGA1, GGA2, and GGA3) in humans with similar trafficking functions. All three GGAs have identical domain organizations, containing the N-terminal Vps27, Hrs, Stam (VHS) domain followed by the GAT (GGAs and TOM1) domain, the hinge region, and the C-terminal GAE (γ-adaptin ear) domain. Each domain of the GGAs has been shown to interact with specific proteins to coordinate their trafficking functions. Specifically, the N-terminal VHS domain interacts with the DXXLL-type sorting motifs of cargo proteins that cycle between the TGN and the endosomal compartment (8–17). These highly coordinated VHS-DXXLL signal interactions specifically dictate cargo proteins into the TGN-to-endosome pathway.

It has been known that APs play an important role in the endocytic trafficking and lysosomal sorting of agonist-occupied GPCRs (7, 18–20) whereas Hrs modulates the recycling process of internalized GPCRs (21, 22). However, the function of GGAs in any trafficking processes of the GPCR superfamily has not been studied. To elucidate the molecular mechanisms underlying the cell surface targeting of newly synthesized GPCRs, here we have determined the role of GGA3 in the export trafficking of α_2-adrenergic receptors (α_2-ARs), prototypic GPCRs that have three subtypes (α_{2A}-AR, α_{2B}-AR, and α_{2C}-AR). We have demonstrated that GGA3 is required for the TGN-to-cell surface transport of α_{2B}-AR, which is mediated through a specific interaction. These data have identified a novel function for GGA3 in the plasma membrane receptor transport *en route* from the TGN.

MATERIALS AND METHODS

Plasmid constructions. α_{2B}-ARs tagged with either green fluorescent protein (GFP) at the C terminus, encoded by the pEGFP-N1 vector (α_{2B}-

Received 5 January 2016 Accepted 20 January 2016

Accepted manuscript posted online 25 January 2016

Citation Zhang M, Davis JE, Li C, Gao J, Huang W, Lambert NA, Terry AV, Jr, Wu G. 2016. GGA3 interacts with a G protein-coupled receptor and modulates its cell surface export. Mol Cell Biol 36:1152–1163. doi:10.1128/MCB.00009-16.

Address correspondence to Guangyu Wu, guwu@gru.edu.

M.Z. and J.E.D. contributed equally to this work.

Supplemental material for this article may be found at http://dx.doi.org/10.1128/MCB.00009-16.

AR-GFP), or three hemagglutinins (HA) (YPYDVPDYA) at the N terminus, encoded by the pcDNA3.1(−) vector (HA-α_{2B}-AR), were generated as described previously (23, 24). The glutathione *S*-transferase (GST) fusion protein constructs comprising the first intracellular loop (ICL1, residues 44 to 53), the second one (ICL2, residues 117 to 131), and the third one (ICL3, residues 205 to 369), different lengths of ICL3 (K205 to P284, R285 to E369, R285 to C326, N327 to E369, N327 to L348, L339 to Q359, and G349 to E369), and the C terminus (residues 430 to 453) of α_{2B}-AR were generated using the pGEX-4T-1 vector as described previously (23, 24), and a similar strategy was used to generate the GST fusion protein construct comprising ICL3 of α_{2A}-AR. Full-length GGA3 tagged with myc at its N terminus was generously provided by Juan S. Bonifacino (Eunice Kennedy Shriver National Institute of Child Health and Human Development, NIH). Arrestin-3 and its dominant negative mutant arrestin-3(201–409) were obtained from Jeffrey L. Benovic (Thomas Jefferson University). The GST fusion protein construct comprising the VHS domain of GGA3 was from Addgene (Cambridge, MA) as described previously (25). To generate GFP-tagged GGA3 and its domains (VHS, residues 1 to 146; GAT, residues 147 to 313; hinge, residues 314 to 493; and GAE, residues 595 to 723), the coding sequence for each was generated by PCR and then cloned into the pEGFP-C1 vector. α_{2B}-AR and GGA3 mutants were generated using the QuikChange site-directed mutagenesis kit (Agilent Technologies).

Cell culture and transient transfection. HEK293, HeLa, MCF7, and HT29 cells were cultured as described previously (26, 27). Transient transfection of cells was carried out using Lipofectamine 2000 reagent (ThermoFisher Scientific) (28). The transfection efficiency was estimated to be greater than 70% based on the GFP fluorescence.

Generation of inducible cell lines expressing α_{2B}-AR. In order to study newly synthesized α_{2B}-AR and to characterize its cell surface transport over the time, the Tet-On 3G tetracycline-inducible gene expression system (Clontech Laboratories, Inc.) was utilized to generate stable cell lines inducibly expressing HA-α_{2B}-AR in HEK293 cells. Briefly, HA-α_{2B}-AR was cloned into the pTRE3G-TRES vector at the BglII and ClaI restriction sites and cotransfected with the PLKO.1 vector. Single-cell colonies were selected by incubation with puromycin for 2 weeks and amplified. Intact cell ligand binding assays as described below were used to detect α_{2B}-AR expression at the cell surface. A total of 8 cell lines inducibly expressing HA-α_{2B}-AR ranging from 1.3×10^5 to 8.5×10^5 receptors per cell were generated. The cell line expressing HA-α_{2B}-AR at the highest level was utilized in the current study.

Depletion of GGA3. Short hairpin RNA (shRNA) targeting GGA3 (356 AATTCCTGTGGATAGGACGCT 376) was kindly provided by Stuart Kornfeld (Washington University School of Medicine) as described previously (29). For shRNA-mediated knockdown of GGA3, cells cultured on 6-well plates were transiently transfected with 2.0 μg of control or GGA3 shRNA for 24 h. The cells were split into 12 wells at a density of 5×10^5 cells per well and cultured for an additional 24 h. For small interfering RNA (siRNA)-mediated knockdown of GGA3 in cells, two Stealth RNAi duplexes (siRNA) targeting human GGA3 (1703 TGTGAC AGCCTACGATAAA 1721) as described previously (30) were synthesized. To generate siRNA-resistant GGA3, two primers (5′-TGCCCTTC CTGTGACTGCGTATGACAAGAACGGCTTCCGCATC-3′ and 5′-GA TGCGGAAGCCGTTCTTGTCATACGCAGTCACAGGAAGG GCA-3′) were used in the mutagenesis reactions using GFP-GGA3 as a template. A, C, C, T, and A in positions 1709, 1712, 1715, 1718, and 1721 in the nucleotide sequence of the construct GGA3 were mutated to T, G, T, C, and G, respectively, to achieve siRNA resistance without changing the encoded amino acid sequence.

Ligand binding of intact live cells. The cell surface expression of α_2-ARs was measured by ligand binding of intact live cells using the cell-nonpermeable radioligand [^{3}H]RX821002 (2-methoxyidazoxan) as described previously (23, 24). Briefly, cells were incubated with Dulbecco's modified Eagle medium (DMEM) plus [^{3}H]RX821002 (20 nM) in a total volume of 400 μl for 90 min. The nonspecific binding of α_2-ARs was determined in the presence of rauwolscine (10 μM). The binding was terminated, and excess radioligands were eliminated by washing the cells with ice-cold DMEM. The retained radioligands were then extracted by digesting the cells in 1 M NaOH for 2 h. The radioactivity was counted by liquid scintillation spectrometry. To measure the maximum number of binding sites (B_{max}) and equilibrium dissociation constant (K_D) values of α_{2B}-AR, HEK293 cells inducibly expressing HA-α_{2B}-AR were incubated with different concentrations of [^{3}H]RX821002 (0.5, 1, 2, 3, 4, 5, 7.5, 10, 20, and 30 nM) after induction with doxycycline at a concentration of 40 ng/ml for 24 h. In another set of experiments, the cells cultured and incubated with doxycycline under the same conditions were used for preparation of membrane proteins without incubation with the radioligand as described previously (31). For measurement of endogenous α_2-ARs, MCF7 and HT29 cells were cultured on 6-well dishes and transfected with GGA3 shRNA or siRNA for 48 h. For measurement of α_{2B}-AR internalization, HEK293 cells stably expressing α_{2B}-AR were cultured on 6-well dishes and transfected with control or GGA3 shRNA together with 1 μg of arrestin-3 for 24 h. After starvation for 3 h, the cells were stimulated with epinephrine (100 μM). The cells were washed 3 times, and α_{2B}-AR cell surface expression was measured by intact cell ligand binding at 4°C.

Flow cytometric analysis of receptor expression. Total receptor expression was measured by flow cytometry as described previously (32). Briefly, HEK293 cells expressing HA-α_{2B}-AR were suspended in phosphate-buffered saline (PBS) containing 1% fetal calf serum at a density of 4×10^6 cells/ml and permeabilized with 0.2% Triton X-100 in PBS for 5 min on ice. The cells were then incubated with high-affinity anti-HA-fluorescein (3F10) (2 μg/ml) at 4°C for 30 min. After two washings with 0.5 ml of PBS, the fluorescence was analyzed on a flow cytometer (Dickinson FACSCalibur).

Fluorescence microscopy. HEK293 cells were grown on coverslips precoated with poly-L-lysine in 6-well plates and transfected with 50 ng of α_{2B}-AR-GFP together with 400 ng of control or GGA3 shRNA. The cells were permeabilized with PBS containing 0.2% Triton X-100 for 5 min and blocked with 5% normal donkey serum for 1 h. The cells were then incubated with antibodies against p230 (1:100 dilution) for 1 h. After washing with PBS (3 times for 5 min), the cells were incubated with Alexa Fluor 594-labeled secondary antibody (1:2,000 dilution) for 1 h. Images were captured using an LSM510 Meta Zeiss confocal microscope as described previously (24, 33). To detect the cell surface expression of inducibly expressed HA-α_{2B}-AR, the cells were stained with anti-HA antibodies (1:500 dilution) without permeabilization. To study the subcellular localization of GGA3, HeLa cells cultured in 6-well dishes were transfected with 200 ng of GFP-tagged GGA3 and then stained with antibodies against GM130, a Golgi body marker.

Measurement of ERK1/2 activation. HEK293 cells inducibly expressing α_{2B}-AR were cultured in 6-well dishes and transfected with GGA3 siRNA or shRNA for 36 h. The cells were then incubated with tetracycline at 40 ng/ml for 24 h. After starvation for at least 3 h, the cells were stimulated with UK14304 for 5 min. In some experiments, the cells stimulated with phorbol-12-myristate-13-acetate (PMA) at a concentration of 1 μM for 5 min were used as a positive control. To measure extracellular signal-regulated kinase 1/2 (ERK1/2) activation by endogenous α_2-ARs, cells were transfected with GGA3 siRNA for 36 h and then stimulated with UK14304 as above. Stimulation was terminated by addition of 1× SDS-loading buffer. ERK1/2 activation was determined by immunoblotting using phospho-specific ERK1/2 antibodies (Santa Cruz) as described previously (28).

Measurement of cAMP production. Cyclic AMP (cAMP) concentrations were measured by using the Cyclic AMP XP Assay kit (Cell Signaling Technology) as described previously (26). Briefly, HEK293 cells inducibly expressing α_{2B}-AR were cultured in 6-well dishes and transfected with GGA3 siRNA or shRNA for 36 h and then incubated with tetracycline at 40 ng/ml for 24 h. The cells were then split into 96-well plates at a density of 1×10^4 cells/well. After starvation for 1 h, the cells were stimulated with forskolin (1 μM) with or without different concentrations of UK14304

(10 to 1,000 nM) in the presence of 0.1 mM isobutylmethylxanthine for 5 min at 37°C. The reactions were stopped by aspirating the medium, and the cells were lysed with 100 μl of lysis buffer. Fifty microliters of cell lysate was transferred into microtiter plates, and cAMP concentrations were measured according to the protocol provided by the kit.

Protein-protein interaction assays. For coimmunoprecipitation (co-IP), HEK293 cells inducibly expressing HA-α_{2B}-AR were cultured on 100-mm dishes and transfected with 10 μg of GFP-GGA3 for 24 h. After incubation with doxycycline (40 ng/ml) for 24 h, the cells were washed twice with PBS, harvested, and lysed with 1 ml of lysis buffer (50 mM Tris-HCl [pH 7.4], 150 mM NaCl, 1% Nonidet P-40, 0.01% SDS, and Complete Mini protease inhibitor mixture). After gentle rotation for 1 h, samples were centrifuged for 15 min at 14,000 × *g*, and the supernatant was incubated with 50 μl of Dynabeads protein G for 1 h at 4°C to remove nonspecific bound proteins. Samples were then incubated with 2 μg of anti-α_{2B}-AR antibodies overnight at 4°C with gentle rotation followed by incubation with 50 μl of Dynabeads protein G for 4 h. The beads were washed 3 times with lysis buffer without SDS. Immunoprecipitated proteins were eluted with 30 μl of SDS-gel loading buffer and separated by SDS-PAGE. GFP-GGA3 and HA-α_{2B}-AR in the IP were detected by immunoblotting using GFP and α_{2B}-AR antibodies, respectively. For co-IP of α_{2B}-AR and endogenous GGA3, two 100-mm dishes of HEK293 cells were transfected with α_{2B}-AR or its mutant for 48 h and co-IP assays were carried out using α_{2B}-AR antibodies as described above.

For GST fusion protein pulldown assays, the GST fusion proteins were expressed in bacteria and purified as described previously (23, 24). GST fusion proteins immobilized on the glutathione resin were either used immediately or stored at 4°C for no longer than 3 days. GST fusion proteins tethered to the glutathione resin were incubated with total cell lysates in 500 μl of binding buffer (20 mM Tris-HCl [pH 7.5], 1% NP-40, 140 mM NaCl, and 1 mM $MgCl_2$) at 4°C for 4 to 6 h. The resin was washed 4 times with 0.5 ml of binding buffer, and the retained proteins were solubilized in SDS-gel loading buffer and separated by SDS-PAGE. Proteins bound to GST fusion proteins were detected by immunoblotting.

For GGA3 interaction with peptide-conjugated agarose beads, the peptide NH2-GKNVGVASGQWWRRRTQLSRE-COOH derived from the α_{2B}-AR ICL3 and its mutant NH2-GKNVGVASGQWWAAATQLSR E-COOH, in which RRR were mutated to AAA, were synthesized, purified by high-performance liquid chromatography (HPLC) to >75%, and directly conjugated to agarose beads by Biosynthesis Inc. (Lewisville, TX). The peptide-conjugated agarose beads (10 μl, approximately 13 μmol peptides) were incubated with 500 μg of cell lysate prepared from HEK293 cells transfected with the GFP-tagged GGA3 VHS domain in 500 μl of binding buffer (20 mM Tris-HCl [pH 7.4], 2% NP-40, 140 mM NaCl) at 4°C overnight. The resin was washed 4 times, and the retained proteins were solubilized in 1× SDS gel loading buffer and separated by SDS-PAGE. Bound proteins were detected by immunoblotting using anti-GFP antibodies. To study the direct interaction between the α_{2B}-AR ICL3 and the GGA3 VHS domain, the VHS domain and its mutant were generated as GST fusion proteins, eluted from the glutathione beads, and incubated with ICL3 peptide-conjugated agarose as described above. Bound proteins were detected by immunoblotting using anti-GST antibodies.

Statistical analysis. Differences were evaluated using Student's *t* test, and *P* values of <0.05 were considered statistically significant. Data are expressed as the means ± standard errors (SE).

RESULTS

Characterization of cell lines inducibly expressing α_{2B}-AR. The stable HEK293 cells generated by using the Tet-On 3G inducible expression system to drive the expression of HA-α_{2B}-AR were incubated with increasing concentrations of doxycycline for 24 h or incubated with doxycycline at a concentration of 40 ng/ml for different time periods, and the numbers of α_{2B}-AR at the cell surface were determined by intact cell ligand binding. Doxycycline dose-dependent and incubation time-dependent expression of α_{2B}-AR are shown in Fig. 1A and B, respectively. α_{2B}-AR expression at the cell surface was clearly detectable after 6 h induction with doxycycline at the saturating concentration of 40 ng/ml and reached a plateau after 20 h of induction. The time required to achieve 50% of the maximal receptor expression at the cell surface ($t_{1/2}$) was approximately 10.6 h after induction. Consistent with ligand binding data, robust expression of α_{2B}-AR at the cell surface was observed by confocal microscopy following staining with anti-HA antibodies in nonpermeabilized cells after treatment with doxycycline whereas α_{2B}-AR expression was undetectable in cells

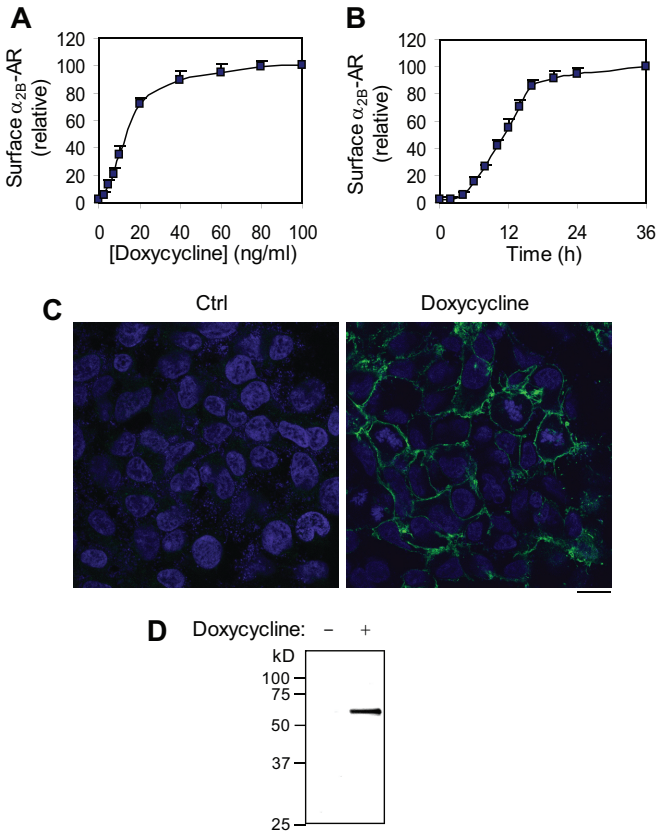

FIG 1 Inducible expression of α_{2B}-AR in HEK293 cells. (A) Doxycycline dose-dependent induction of cell surface α_{2B}-AR expression. The cells were incubated with different concentrations of doxycycline for 24 h, and the cell surface α_{2B}-AR expression was quantified by intact cell ligand binding using [^{3}H]RX821002 at 20 nM. The data shown are percentages of specific binding obtained from cells treated with doxycycline (100 ng/ml), in which the mean value of specific [^{3}H]RX821002 binding was 35,672 ± 797 cpm per well (n = 3). (B) Doxycycline time-dependent induction of cell surface α_{2B}-AR expression. HEK293 cells were incubated with doxycycline (40 ng/ml) for different time periods. The data shown are percentages of specific binding obtained from cells after induction for 36 h, in which the mean value of specific ligand binding was 36,123 ± 573 cpm per well (n = 3). (C) Detection of cell surface HA-α_{2B}-AR expression by confocal microscopy. HEK293 cells were incubated with or without doxycycline (40 ng/ml) for 24 h and stained with anti-HA antibodies in nonpermeabilized cells. Green, HA-α_{2B}-AR; blue, DNA staining by 4′,6-diamidino-2-phenylindole (DAPI). Bar, 10 μm. (D) Detection of HA-α_{2B}-AR expression by immunoblotting. HEK293 cells were incubated with or without doxycycline (40 ng/ml) for 24 h. Total cell lysates (50 μg) were separated by SDS-PAGE, and HA-α_{2B}-AR expression was measured by immunoblotting using α_{2B}-AR antibodies. Similar results were obtained in 3 experiments.

that had not been incubated with doxycycline (Fig. 1C). Doxycycline-induced expression of HA-α_{2B}-AR was further confirmed by immunoblotting using α_{2B}-AR antibodies (Fig. 1D).

Effect of depleting GGA3 on the cell surface transport of α_2-ARs. We then determined the effect of short hairpin RNA (shRNA)-mediated depletion of endogenous GGA3 on the cell surface expression of inducibly expressed α_{2B}-AR. The introduction of GGA3 shRNA markedly knocked down GGA3 (by 92%) compared with cells transfected with control shRNA (see Fig. S1A in the supplemental material). shRNA-mediated knockdown of GGA3 moderately but significantly attenuated the magnitude of α_{2B}-AR expression at the cell surface after doxycycline induction for more than 12 h (Fig. 2A). The maximal inhibition (approximately 30%) was observed after doxycycline induction for more than 20 h, and $t_{1/2}$ values were 10.8 and 10.9 h in cells transfected with control and GGA3 shRNA, respectively (Fig. 2A). The radioligand saturation binding curves showed that GGA3 knockdown significantly reduced the B_{max} but not K_D of α_{2B}-AR (Fig. 2B).

GGA3 is a TGN-localized protein, and shRNA-mediated knockdown of GGA3 was shown to disrupt the localization of β-GalT, a *trans*-Golgi marker, in HeLa cells (29). To determine if the effect of shRNA-mediated GGA3 knockdown on the cell surface expression of α_{2B}-AR was induced by disruption of the TGN/Golgi body integrity, which may produce nonspecific effects on global protein transport, we determined the effect of GGA3 knockdown by siRNA that were shown to have no effect on the TGN structure (30). siRNA-mediated knockdown of GGA3 inhibited the cell surface expression of inducibly expressed α_{2B}-AR, and this inhibition was completely reversed by expression of an siRNA-resistant form of GGA3 (Fig. 2C; see also Fig. S1B in the supplemental material). Similar to α_{2B}-AR, the cell surface expression of α_{2C}-AR was also significantly attenuated, whereas the transport of α_{2A}-AR was not affected by GGA3 siRNA in HEK293 cells transiently transfected with the receptors (Fig. 2C). In contrast, GGA3 knockdown did not affect the overall synthesis of α_{2B}-AR as measured by flow cytometry (Fig. 2D) and by immunoblotting (Fig. 2E). Furthermore, GGA3 overexpression did not influence the cell surface expression of α_{2B}-AR (see Fig. S2A in the supplemental material), suggesting that expression of endogenous GGA3 is not a rate-limiting factor for the cell surface expression of α_{2B}-AR.

To eliminate the possibility that the reduction of the cell surface expression of α_{2B}-AR caused by GGA3 knockdown was induced by enhanced constitutive internalization of the receptor, we determined if expression of dominant negative mutant of arrestin-3, which has been shown to control the internalization process of α_{2B}-AR (34), could reverse the inhibitory effects. Expression of the dominant negative mutant arrestin-3(201–409) did not influence the cell surface expression of α_{2B}-AR in cells expressing control or GGA3 shRNA (see Fig. S2B in the supplemental material). Furthermore, GGA3 shRNA also did not influence the internalization of α_{2B}-AR in response to epinephrine stimulation (Fig. 2F). These data suggest that GGA3 does not play a major role in the internalization of α_{2B}-AR.

We next determined the role of GGA3 in the cell surface transport of endogenous α_2-ARs in breast cancer MCF7 cells, which express α_{2B}-AR and α_{2C}-AR (35), and in colon cancer HT29 cells, which express only α_{2A}-AR (36). Similar to their inhibitory effects on inducibly expressed α_{2B}-AR, shRNA- and siRNA-mediated knockdown of GGA3 decreased the cell surface expression of α_2-ARs in MCF7 cells by about 40% (Fig. 2G, left panel). In contrast, GGA3 siRNA did not alter the cell surface expression of α_{2A}-AR in HT29 cells (Fig. 2G, right panel). Altogether, these results demonstrate that the normal function of GGA3 is required for the cell surface export of exogenously transfected and endogenous α_{2B}-AR and α_{2C}-AR but not α_{2A}-AR.

Effect of GGA3 knockdown on α_2-AR-mediated signaling. All three α_2-ARs couple to the Gi/Go family G proteins, and their activation has been well shown to stimulate the mitogen-activated protein kinases (MAPK) ERK1/2, inhibit adenylyl cyclases, and suppress voltage-gated calcium channels (24, 26, 37–39). To investigate if GGA3 knockdown-induced reduction of cell surface α_{2B}-AR expression could result in a concomitant defective signaling, the activation of ERK1/2 and the reduction of cAMP production were chosen as functional readouts. Consistent with their abilities to inhibit receptor cell surface transport, transient expression of siRNA targeting GGA3 significantly reduced α_{2B}-AR-mediated ERK1/2 activation in response to UK14304 stimulation in cells inducibly expressing α_{2B}-AR compared to cells transfected with control siRNA (Fig. 3A and B). Similarly, siRNA-mediated depletion of GGA3 (see Fig. S1D in the supplemental material) inhibited the activation of ERK1/2 by endogenous α_2-ARs by 48% in MCF7 cells (Fig. 3C and D). In contrast, GGA3 siRNA did not affect the activation of ERK1/2 by exogenously transfected α_{2A}-AR in HEK293 cells and by endogenous α_{2A}-AR in HT29 cells (see Fig. S1C and E and S3 in the supplemental material). Furthermore, siRNA-mediated GGA3 knockdown reduced the ability of α_{2B}-AR activation to inhibit the cAMP production in response to stimulation with forskolin (Fig. 3E). Similar to GGA3 knockdown by siRNA, shRNA-mediated GGA3 depletion significantly attenuated ERK1/2 activation and cAMP reduction in response to UK14304 stimulation in HEK293 cells inducibly expressing α_{2B}-AR (see Fig. S4 in the supplemental material). These data suggest that GGA3 modulates not only the cell surface transport but also the function of α_{2B}-AR.

GGA3 regulates α_{2B}-AR transport from the TGN. We next determined the effect of GGA3 knockdown on the subcellular distribution of α_{2B}-AR in HEK293 cells by confocal microscopy. As expected, α_{2B}-AR was robustly expressed at the cell surface in cells transfected with control shRNA. In contrast, α_{2B}-AR was clearly arrested in the intracellular compartments, unable to transport to the cell surface, in GGA3 knockdown cells (Fig. 4A).

To define the intracellular compartment in which GGA3 regulates α_{2B}-AR transport, α_{2B}-AR was colocalized with different intracellular organelle markers in cells expressing GGA3 shRNA. The intracellularly accumulated α_{2B}-AR was extensively colocalized with the TGN marker p230 (Fig. 4B) but not with the ER marker DsRed2-ER (see Fig. S5 in the supplemental material) in HEK293 cells transfected with GGA3 shRNA. These data suggest that GGA3 likely controls the cell surface transport of α_{2B}-AR en route from the TGN.

GGA3 interacts with the ICL3 of α_{2B}-AR. It has been well defined that the trafficking function of GGA proteins is mediated through their direct interactions with cargo proteins (8–17). To elucidate the possible molecular mechanisms underlying the function of GGA3 in α_{2B}-AR export, we determined if GGA3 and α_{2B}-AR could physically associate to form a complex in co-IP assays using α_{2B}-AR antibodies. GGA3 was clearly detected in the IP of α_{2B}-AR antibodies (Fig. 5A).

All three α_2-ARs have similar structural features: the third in-

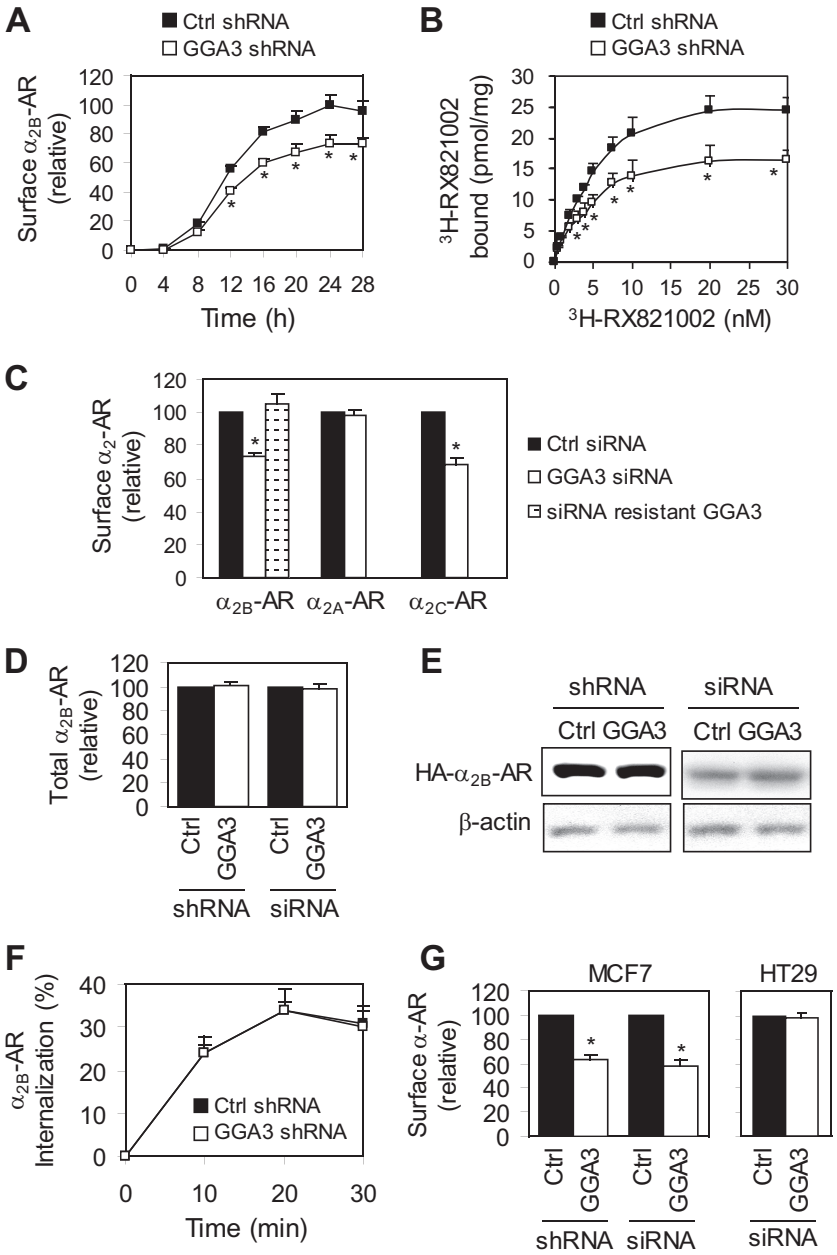

FIG 2 Effects of GGA3 knockdown on the cell surface expression of α_2-ARs. (A) Effect of shRNA-mediated GGA3 knockdown on cell surface α_{2B}-AR expression. HEK293 cells inducibly expressing α_{2B}-AR were transfected with control or GGA3 shRNA and incubated with doxycycline (40 ng/ml) for different time periods. The cell surface α_{2B}-AR expression was determined by intact cell ligand binding using [^{3}H]RX821002 at 20 nM. The data shown are percentages of specific binding obtained from cells transfected with control shRNA and treated with doxycycline for 24 h, in which the mean value of specific ligand binding was 34,408 ± 552 cpm per well ($n = 3$). (B) Effect of shRNA-mediated GGA3 knockdown on the B_{max} and K_D values of α_{2B}-AR. HEK293 cells transfected and treated with doxycycline for 24 h as described above were incubated with different concentrations of [^{3}H]RX821002. In separate experiments, the cells treated under the same conditions were used for membrane protein preparation. The B_{max} values were 24.6 and 16.5 pmol/mg protein in control and GGA3 knockdown cells, respectively ($P < 0.05$, $n = 3$), whereas the K_D values in control and GGA3 knockdown cells were the same (4.1 nM). (C) Effects of siRNA-mediated GGA3 knockdown on the cell surface expression of different α_2-ARs. HEK293 cells inducibly expressing α_{2B}-AR were transfected with control siRNA, GGA3 siRNA, or GGA3 siRNA plus siRNA-resistant GFP-GGA3 (left bars). To determine the effect of GGA3 knockdown on the cell surface transport of α_{2A}-AR and α_{2C}-AR, HEK293 cells were cotransfected with GGA3 siRNA together with α_{2A}-AR (middle bars) or α_{2C}-AR (right bars) ($n = 3$ to 5). (D) Effect of shRNA- and siRNA-mediated knockdown of GGA3 on total α_{2B}-AR expression measured by flow cytometry following staining with HA antibodies in permeabilized cells ($n = 4$). (E) Effect of GGA3 knockdown on total HA-α_{2B}-AR expression measured by immunoblotting using HA antibodies. (F) Effect of depleting GGA3 on α_{2B}-AR internalization. HEK293 cells stably expressing α_{2B}-AR were transfected with GGA3 shRNA and then stimulated with epinephrine (100 μM) ($n = 3$). (G) Effect of GGA3 knockdown on the cell surface expression of endogenous α_2-ARs in MCF7 and HT29 cells measured by intact cell ligand binding. The mean values of specific ligand binding were 462 ± 56 cpm in MCF7 cells transfected with control shRNA, 478 ± 49 cpm in MCF7 cells transfected with control siRNA, and 452 ± 43 in HT29 cells transfected with control siRNA ($n = 3$). *, $P < 0.05$ versus the respective control.

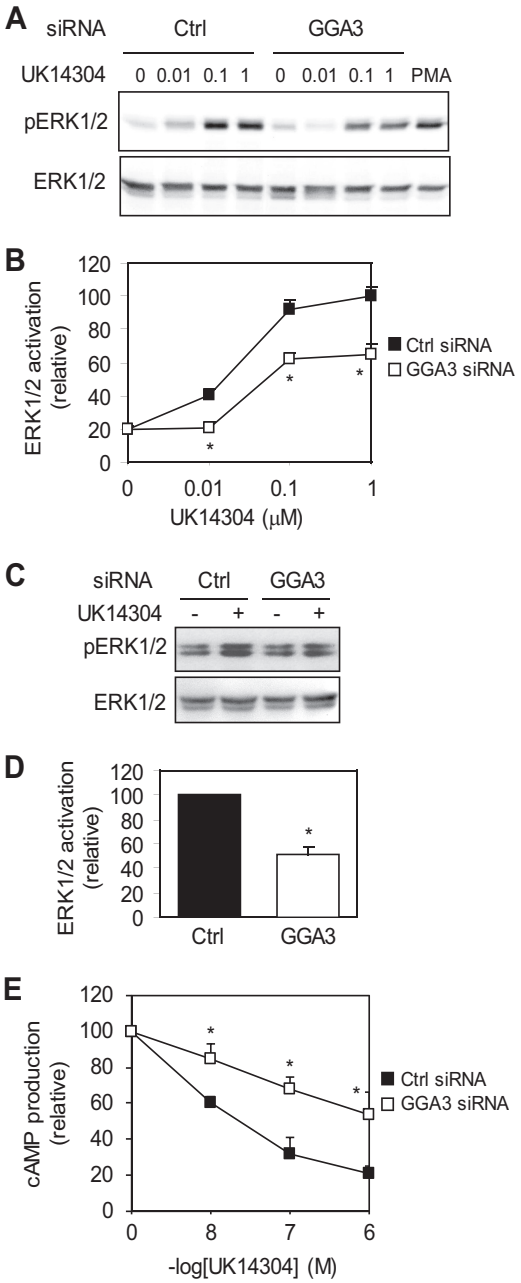

FIG 3 Inhibition of α_{2B}-AR-mediated signaling by depleting GGA3. (A) Effect of GGA3 knockdown on α_{2B}-AR-mediated ERK1/2 activation. HEK293 cells inducibly expressing α_{2B}-AR were transfected with control or GGA3 siRNA and incubated with doxycycline at 40 ng/ml for 24 h. After starvation for 3 h, the cells were stimulated with different concentrations of UK14304 (0.01, 0.1, and 1 μM) for 5 min. The simulation with PMA at 1 μM for 5 min was used as a positive control. (B) Quantitation of data shown in panel A (n = 4). (C) Effect of GGA3 knockdown on ERK1/2 activation by endogenous α_2-ARs. MCF7 cells were transfected with control or GGA3 siRNA for 48 h and stimulated with UK14304 at 1 μM for 5 min. (D) Quantitation of data shown in panel C (n = 3). (E) Effect of GGA3 knockdown on α_{2B}-AR-mediated inhibition of cAMP production. HEK293 cells inducibly expressing α_{2B}-AR were transfected, incubated with doxycycline, and stimulated with forskolin (1 μM) plus different concentrations of UK14304 for 5 min at 37°C (n = 3). The data shown are percentages of the mean values obtained from cells transfected with control siRNA and stimulated with forskolin alone. *, $P < 0.05$ versus the respective control.

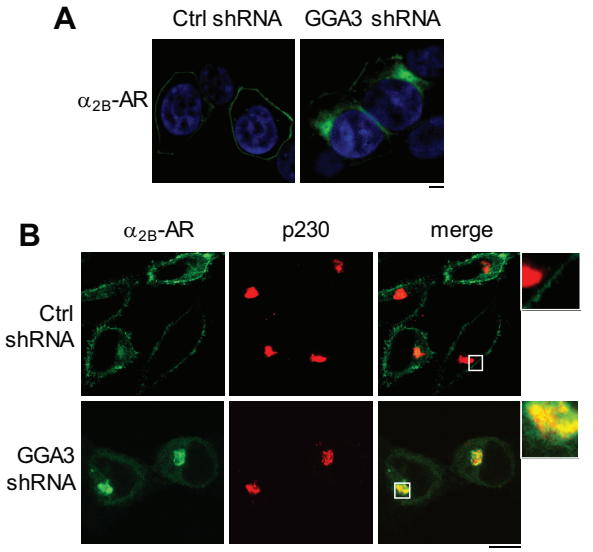

FIG 4 Effect of GGA3 knockdown on subcellular localization of α_{2B}-AR. (A) HEK293 cells were transiently transfected with α_{2B}-AR-GFP together with control or GGA3 shRNA for 48 h. (B) Colocalization of α_{2B}-AR with p230. HEK293 cells were transfected with α_{2B}-AR-GFP together with control or GGA3 shRNA and then stained with anti-p230 antibodies. The images are representative of at least 3 independent experiments. Green, α_{2B}-AR-GFP; red, p230; blue, DNA staining by DAPI (nuclei); yellow, colocalization of α_{2B}-AR-GFP with p230. Bars, 10 μm. Similar results were obtained in 3 to 5 experiments.

tracellular loop (ICL3) is quite large, with more than 170 amino acid residues, whereas other loops and the termini are relatively short, with <25 residues (Fig. 5B). To identify the intracellular domain that mediated α_{2B}-AR interaction with GGA3, ICL1, ICL2, ICL3, and the C terminus of α_{2B}-AR were generated as GST fusion proteins and then incubated with total lysates prepared from cells transiently transfected with myc-GGA3. The GST fusion proteins of the ICL3 but not the ICL1, the ICL2, or the C terminus were capable of interacting with GGA3 (Fig. 5C).

As our preceding data have demonstrated that GGA3 modulates the cell surface transport of α_{2B}-AR but not α_{2A}-AR, we next compared the GGA3 interaction with the ICL3 of α_{2A}-AR and α_{2B}-AR in GST fusion protein pulldown assays. In contrast to α_{2B}-AR, the α_{2A}-AR ICL3 did not interact with GGA3 (Fig. 5D).

α_{2B}-AR interacts with the VHS domain of GGA3. To search for the domain of GGA3 responsible for binding to α_{2B}-AR, the VHS, GAT, hinge, and GAE domains of GGA3 were generated as GFP fusion proteins (Fig. 6A). We first visualized their subcellular distribution by confocal microscopy. Consistent with other reports (14, 25), full-length GGA3 was extensively expressed in the Golgi network. Similarly, the GAT domain was also mainly localized to the Golgi network. The hinge, the VHS, and the GAE domains of GGA3 were largely expressed in the cytoplasm. In addition, the VHS and the GAE domains were seemingly also expressed in the nuclear compartment (Fig. 6B).

We next determined the interaction of individual domains of GGA3 with GST-ICL3 fusion proteins in GST fusion protein pulldown assays. The GGA3 VHS domain, but not the GAT, hinge, or GAE domain, bound to the ICL3 of α_{2B}-AR (Fig. 6C).

We then sought to define if the VHS domain of GGA3 was able to interact with full-length α_{2B}-AR. In this experiment, the VHS

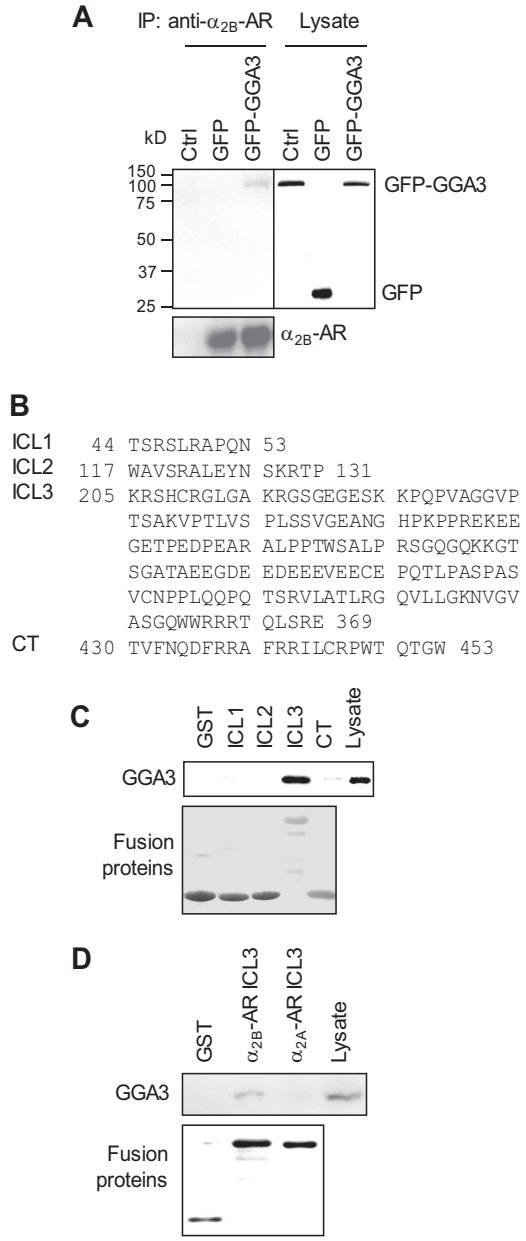

FIG 5 GGA3 interaction with α_{2B}-AR and its ICL3. (A) Interaction of α_{2B}-AR with GGA3 as measured by co-IP assays. HEK293 cells stably expressing HA-α_{2B}-AR were transfected with pEGFP-C1 (GFP) or GFP-tagged GGA3. Normal HEK293 cells transfected with GFP-tagged GGA3 were also used as a negative control (Ctrl). The receptors were immunoprecipitated with α_{2B}-AR antibodies. The amounts of GGA3 (upper panel) and α_{2B}-AR (lower panel) were determined by immunoblotting using GFP and α_{2B}-AR antibodies, respectively. Lysate, 1% of total input. (B) Sequences of ICL1, ICL2, ICL3, and C terminus (CT) of α_{2B}-AR. (C) Interaction of α_{2B}-AR intracellular domains with GGA3. Myc-GGA3 was expressed in HEK293 cells, and total cell homogenates were incubated with GST fusion proteins. Bound GGA3 was revealed by immunoblotting using myc antibodies (upper panel). Lysate, 5% of total input. (D) Interaction of the ICL3 of α_{2A}-AR and α_{2B}-AR with GGA3 in GST fusion protein pulldown assays as described in panel C. Lysate, 5% of total input. Lower images in panels C and D show Coomassie blue staining of purified GST fusion proteins. Similar results were obtained in at least 3 experiments.

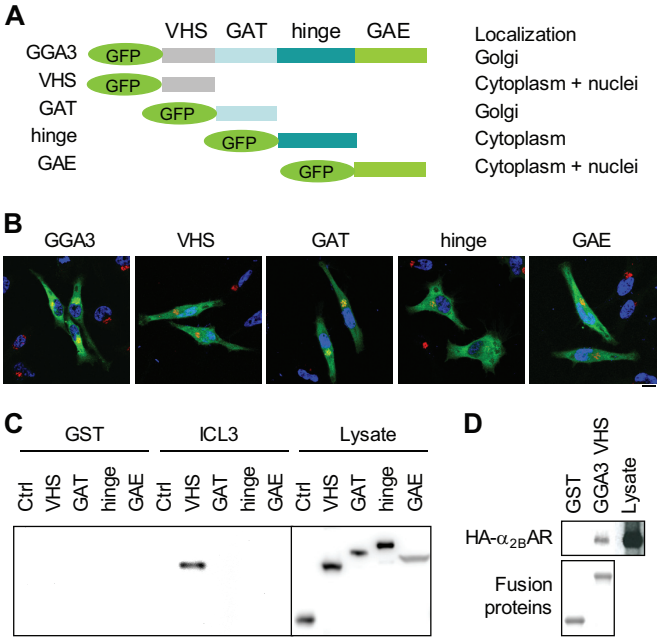

FIG 6 Identification of the α_{2B}-AR-binding domain of GGA3. (A) Diagram showing the generation of GFP-tagged GGA3 and its domains. (B) Subcellular distribution of GGA3 domains. HeLa cells were transfected and stained with antibodies against the Golgi marker GM130. Green, GFP-GGA3; red, GM130; blue, DNA staining by DAPI (nuclei). Bar, 10 μm. (C) Interaction of the α_{2B}-AR ICL3 with different GGA3 domains. The GFP-tagged VHS, GAT, hinge, and GAE domains of GGA3 were expressed in HEK293 cells. Total cell lysates were incubated with GST-ICL3 fusion proteins. Bound GGA3 domains were revealed by immunoblotting using GFP antibodies. Total cell lysates expressing GFP alone were used as a control. (D) α_{2B}-AR interaction with the GGA3 VHS domain. The GGA3 VHS domain was generated as GST fusion proteins and incubated with total cell lysates prepared from HEK293 cells expressing HA-α_{2B}-AR. Bound HA-α_{2B}-AR was detected by immunoblotting using HA antibodies. Lysate, 5% of total input. Similar results were obtained in at least 3 experiments.

domain of GGA3 was generated as GST fusion proteins and its interaction with full-length HA-α_{2B}-AR was determined in GST fusion protein pulldown assays. GST-VHS fusion proteins, but not GST alone, strongly interacted with HA-α_{2B}-AR (Fig. 6D). These data demonstrate that α_{2B}-AR interacts with the VHS domain of GGA3.

Identification of the GGA3-binding site in the α_{2B}-AR ICL3. The progressive deletion strategy was utilized to further identify the GGA3-binding domain in the α_{2B}-AR ICL3 in GST fusion protein pulldown assays. ICL3 was first split into the N-terminal half K205-P284 and the C-terminal half R285-E369. Similar to the entire ICL3, the C-terminal portion R285-E369 strongly interacted with the GGA3 VHS domain, whereas the N-terminal portion K205-P284 did not (Fig. 7A and B). Furthermore, the C-terminal half, but not the N-terminal half, was confirmed to interact with full-length GGA3 (Fig. 7C). A further split of the C-terminal portion revealed that N327-E369, but not R285-C326, interacted with the GGA3 VHS domain. Moreover, the GST fusion proteins with the fragment G349-E369, but not N327-L348 and L339-Q358, interacted with the GGA3 VHS domain (Fig. 7A and B). These data demonstrate that the GGA3-binding site localizes within the G349-E369 domain (Fig. 7A and B).

We have previously demonstrated that the triple Arg (3R) mo-

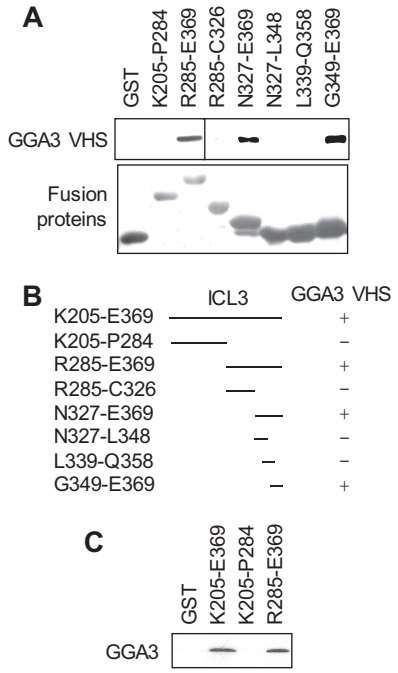

FIG 7 Mapping of the GGA3-binding domain in the α_{2B}-AR ICL3 by progressive deletion. (A) Representative blot showing the interaction of different ICL3 fragments with the GGA3 VHS domain. (B) Summary of progressive deletion to identify the GGA3-binding domain in the ICL3 of α_{2B}-AR as shown in panel A. (C) Interaction of the N- and the C-terminal portions of the α_{2B}-AR ICL3 with full-length GGA3 as measured in GST fusion protein pulldown assays. Similar results were obtained in 3 experiments.

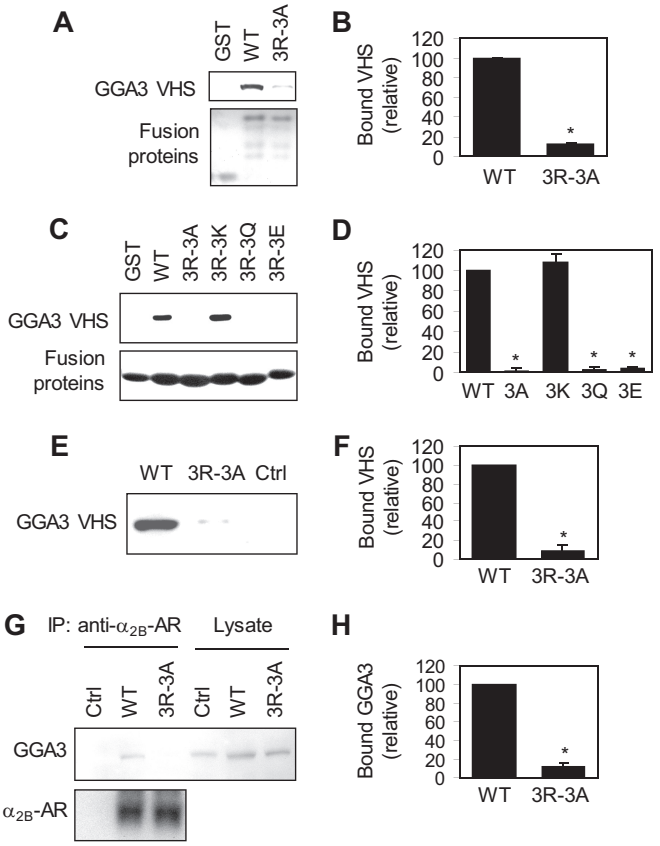

FIG 8 Identification of the triple Arg motif as the GGA3-binding site. (A) Effect of mutating 3R on the interaction of G349-E369 with the GGA3 VHS domain. G349-E369 and its 3R-3A mutant were generated as GST fusion proteins, and their interaction with the GGA3 VHS domain was determined in GST fusion protein pulldown assays. (B) Quantitation of data shown in panel A. (C) Effect of mutating 3R to 3A, 3K, 3Q, and 3E on the ICL3 interaction with the GGA3 VHS domain. (D) Quantitation of data shown in panel C. (E) Interaction of ICL3-conjugated agarose beads with the GGA3 VHS domain. G349-E369 and its mutant 3R-3A were synthesized and conjugated to agarose and then incubated with total cell homogenates prepared from cells expressing GFP-VHS. The bound VHS domain was revealed by immunoblotting using GFP antibodies. (F) Quantitation of data shown in panel E. (G) Interaction of α_{2B}-AR with endogenous GGA3 as measured by co-IP assays. HEK293 cells were transiently transfected with α_{2B}-AR or its mutant 3R-3A. HEK293 cells without transfection were used a negative control (Ctrl). The receptors were immunoprecipitated with α_{2B}-AR antibodies. The amounts of GGA3 (upper panel) and α_{2B}-AR (lower panel) were determined by immunoblotting using GGA3 and α_{2B}-AR antibodies, respectively. Lysate, 2% of total input. (H) Quantitation of data shown in panel G. *, $P < 0.05$ versus WT ($n = 3$ or 4).

tif at positions 361 to 363 in the ICL3 mediates the α_{2B}-AR interaction with the COPII vesicle components Sec24C/D and modulates receptor export from the ER (23). To determine if the 3R motif also mediated the α_{2B}-AR interaction with GGA3, we determined the effect of mutating the 3R motif on the ICL3 interaction with the GGA3 VHS domain. The mutation of three Arg to three Ala (3A) significantly reduced (by 88%) the interaction of the ICL3 fragment G348-E369 with the GGA3 VHS domain (Fig. 8A and B). Similar to the mutation to 3A, the 3R mutation to three noncharged Gln (3Q) or three negatively charged Glu (3E) completely blocked the ICL3 interaction with the GGA3 VHS domain, whereas mutation of 3R to three positively charged Lys (3K) retained the interaction of ICL3 with GGA3 (Fig. 8C and D). These data demonstrate that the positively charged property of the 3R motif is a major determinant for interaction with GGA3.

To exclude the possible interference of GST on the ICL3 interaction with GGA3 and further characterize the interaction, a 21-residue peptide of the ICL3 (from G349 to E369) containing the 3R motif and a mutated peptide in which the 3R motif was mutated to 3A were synthesized and conjugated to agarose. Peptide-conjugated agarose beads were incubated with total cell lysates expressing GFP-VHS. Similar to the results obtained from GST fusion protein pulldown assays, the ICL3 peptide-conjugated agarose beads, but not control agarose beads, strongly bound to the VHS domain, whereas the mutated peptide-conjugated beads only very weakly bound to the VHS domain (Fig. 8E and F).

To determine if α_{2B}-AR is able to interact with endogenous GGA3 and if the interaction is thus mediated through the 3R motif, we compared the interaction of α_{2B}-AR and its 3R-3A mutant with endogenous GGA3 in co-IP assays. GGA3 was detected in the IP of α_{2B}-AR antibodies in cells expressing wild-type α_{2B}-AR but not in cells expressing the mutant 3R-3A (Fig. 8G). These data indicate that the 3R motif mediates α_{2B}-AR interaction with GGA3.

Identification of the α_{2B}-AR-binding motif in the VHS domain of GGA3. To define the α_{2B}-AR-binding site in the GGA3 VHS domain, we focused on the highly negatively charged region EDWE in the VHS domain (Fig. 9A). We first determined the effect of mutating EDWE motif to AAWA on the interaction of the GGA3 VHS domain with the α_{2B}-AR ICL3 in GST fusion protein pulldown assays. Consistent with our previous data, mutation of the 3R motif markedly reduced the interaction of the ICL3 with

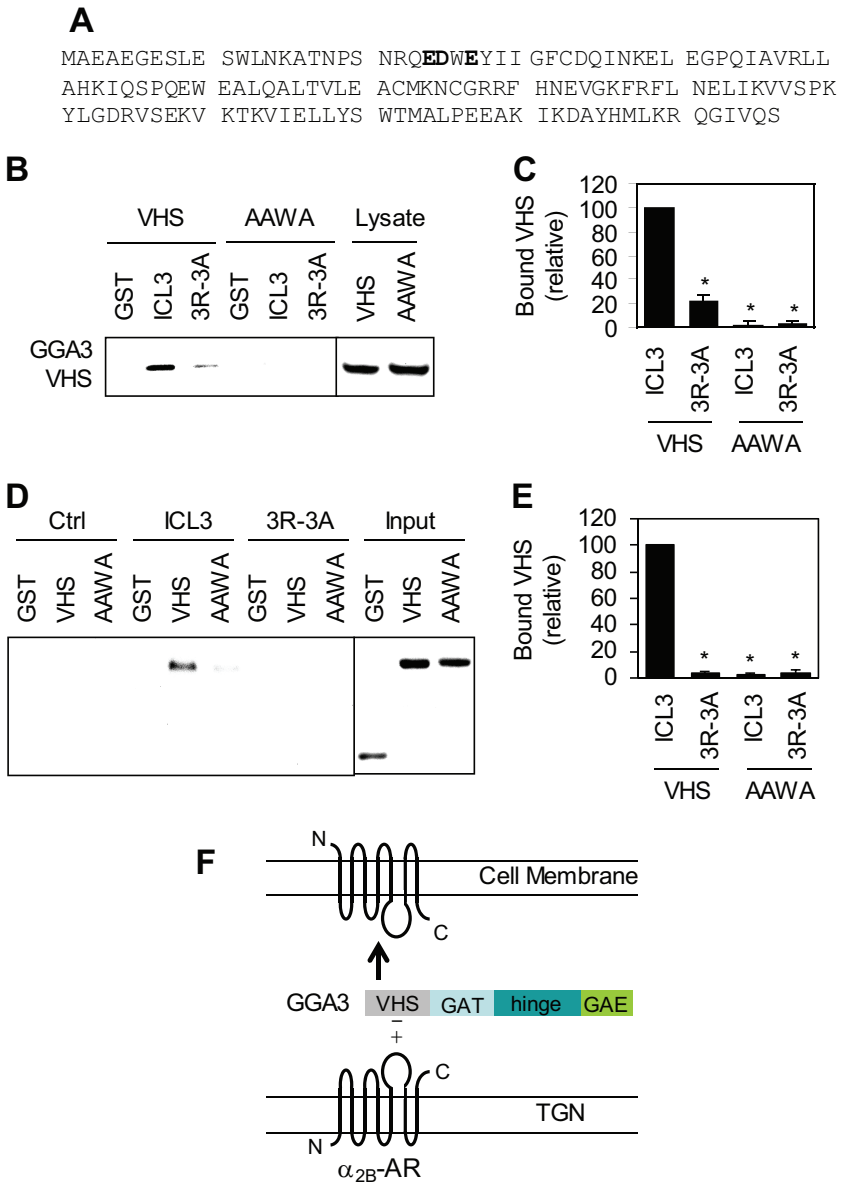

FIG 9 Effect of mutating the acidic motif EDWE on GGA3 interaction with α_{2B}-AR. (A) Sequence of the GGA3 VHS domain. Acidic residues in the motif EDWE that were mutated to Ala (AAWA) are bolded. (B) Effect of mutating EDWE on the interaction of the GGA3 VHS domain with ICL3. ICL3 and its mutant 3R-3A were generated as GST fusion proteins, and the GGA3 VHS domain and its mutant AAWA were tagged with GFP. Their interactions were determined in GST fusion protein pulldown assays. The bound VHS domain was revealed by immunoblotting using GFP antibodies. Lysate, 5% of total input. (C) Quantitation of data shown in panel B ($n = 3$). (D) Motif-mediated direct interaction between α_{2B}-AR and GGA3. The GGA3 VHS domain and its mutant were generated as GST fusion proteins, eluted, and incubated with agarose beads conjugated with ICL3 or its mutant 3R-3A as described in the legend to Fig. 8E. Bound VHS domain was revealed by immunoblotting using GST antibodies. Input, 5% of total input. (E) Quantitation of data shown in panel D ($n = 3$). *, $P < 0.05$ versus the interaction between ICL3 and VHS. (F) Diagram showing the function of GGA3 in regulating α_{2B}-AR plasma membrane transport, which is likely mediated through an ionic interaction between the negatively charged EDWE motif in the VHS domain of GGA3 and the positively charged 3R motif in ICL3 of α_{2B}-AR.

the GGA3 VHS domain. Mutation of the motif EDWE to AAWA abolished the interaction of the GGA3 VHS domain with both wild-type ICL3 and the 3R-3A mutant (Fig. 9B and C). These data demonstrate that the acidic EDXE motif in the GGA3 VHS domain represents a specific α_{2B}-AR-binding site.

To further determine if the interaction between α_{2B}-AR and GGA3 is direct, the GGA3 VHS domain and its mutant EDWE-AAWA were purified as GST fusion proteins and then incubated with the ICL3 peptide-conjugated agarose beads as described above (Fig. 8E). The wild-type VHS domain interacted with the wild-type ICL3 peptide, and mutation of either 3R or EDWE abolished the interaction (Fig. 9D and E). These data suggest that the interaction between α_{2B}-AR and GGA3 is direct and mediated by specific motifs.

DISCUSSION

The most important finding presented here is that we have identified a novel function for GGA3 as an important modulator in the

cell surface transport of α_{2B}-AR, a prototypic GPCR, from the TGN and that the function of GGA3 in the trafficking of α_{2B}-AR is likely mediated through a specific interaction (Fig. 9F).

The GGA family proteins have been well defined to function as adaptors for clathrin-coated vesicles to specifically mediate the transport from the TGN to the endosomal compartment. Our studies have demonstrated that GGA3 plays an important role in the export trafficking of α_{2B}-AR. First, depleting GGA3 by shRNA and siRNA significantly reduced the cell surface expression of α_{2B}-AR as quantified by ligand binding of intact live cells. As ligand binding assays were carried out to measure the numbers of inducibly expressed α_{2B}-AR at the cell surface using the antagonist RX821002 and GGA3 knockdown did not alter the internalization of α_{2B}-AR, the reduction of cell surface receptors caused by GGA3 knockdown reflects the defective export of newly synthesized and fully maturated receptors rather than an augmented internalization of the receptors from the cell surface. In addition, the cell surface expression of endogenous α_2-ARs in MCF7 cells was also inhibited by GGA3 knockdown. However, the inhibitory effects caused by depleting GGA3 were moderate (inhibiting by less than 40%), which is well consistent with other reports demonstrating that depleting a specific component of the transport machinery produced only mild inhibition on the cell surface transport of GPCRs (23, 24). The simplest explanation for this could be that there are multiple pathways to direct α_{2B}-AR export from the Golgi body to the cell surface and GGA3 regulates only one of these pathways that mediate α_{2B}-AR forward transport. We have also shown that, similar to α_{2B}-AR, the cell surface transport of α_{2C}-AR was inhibited by GGA3 knockdown. Surprisingly, α_{2A}-AR cell surface expression was not affected by GGA3, suggesting that GGA3 has selectivity for different α_2-ARs.

Second, GGA3 knockdown induced an extensive accumulation of α_{2B}-AR in the TGN compartment. These data imply that GGA3 is involved in the plasma membrane receptor transport *en route* from the TGN. These data are also consistent with the Golgi body/TGN localization of GGA3 as well as its well-established function in post-Golgi transport. Our previous studies have shown that α_{2B}-AR exit from the Golgi body is dictated by the N-terminal YS motif and its transport from the Golgi body to the cell surface is regulated by Ras-like small GTPases, including Rab8 (33), Rab26 (24), and ARF1 (40), suggesting that multiple regulatory proteins are involved in the post-Golgi traffic of α_{2B}-AR. These results, together with other studies (41, 42), have demonstrated that GPCR export from the Golgi body to the cell surface is a highly regulated and dynamic process.

Third, GGA3 knockdown-induced reduction of α_{2B}-AR transport to the cell surface was in parallel with attenuated receptor signaling measured as ERK1/2 activation and cAMP reduction in response to stimulation with the agonist UK14304. Furthermore, we have shown that GGA3 knockdown, which did not influence α_{2A}-AR cell surface transport, did not affect α_{2A}-AR-mediated ERK1/2 activation. In addition, GGA3 knockdown had no effect on forskolin-stimulated cAMP production in the absence of UK14304. These data strongly suggest that the inhibition of α_{2B}-AR-mediated signaling is most likely caused by the decrease of receptor transport to the cell surface.

It has been well described that the function of GGAs in sorting proteins into the TGN-to-endosome pathway is tightly controlled by the interaction, via their VHS domains, with the DXXLL-type motifs presented in cargos. These cargo proteins include cation-dependent and cation-independent mannose 6-phosphate receptors (9, 11, 14, 15, 17), sortilin (13, 16), sorting-protein-related receptor (12, 43), low-density lipoprotein receptor-related proteins, and β-secretase (8, 10, 16). We have demonstrated that GGA3 and α_{2B}-AR physically associated in co-IP and GST fusion protein pulldown assays. Furthermore, consistent with its function in regulating protein transport, the GGA3 VHS domain is responsible for the interaction with α_{2B}-AR. We have further used the progressive deletion and mutagenesis strategies to successfully identify their interaction sites. We have found that mutation of the 3R motif profoundly reduced α_{2B}-AR interaction with GGA3, specifically the VHS domain. These data suggest that the 3R motif is a novel GGA3-binding signal that controls, at least in part, α_{2B}-AR interaction with GGA3. We have also identified the acidic motif EDWE in the GGA3 VHS domain, which mediates the GGA3 interaction with α_{2B}-AR, indicating that the interaction between α_{2B}-AR and GGA3 is ionic in nature. These data also suggest that regulation of α_{2B}-AR trafficking by GGA3 is highly specific. To the best of our knowledge, α_{2B}-AR is the only cargo molecule identified thus far that interacts with GGA3 through a charged motif. It is possible that GGA3 interaction with the 3R motif of α_{2B}-AR directs the receptor into the plasma membrane transport pathway (Fig. 9F), whereas its interaction with cargo proteins bearing the DXXLL-type signals controls the TGN-to-endosome transport pathway. This possibility is also supported by the fact that the cell surface transport of α_{2C}-AR, which has the RRK motif, is regulated by GGA3, whereas the cell surface transport of α_{2A}-AR, which does not have the triple basic motif (but has the sequence RWR instead), is not mediated through GGA3. It is also interesting that the triple basic motif is highly conserved in the ICL3 of many GPCRs, such as muscarinic receptors (subtypes 1, 2, 3, and 5) and serotonin receptors (subtypes 1A, 1B, 1D, and 2C), as described in our previous publication (23). Therefore, GGA3 may regulate the cell surface transport of these GPCRs.

We have previously demonstrated that the 3R motif in the ICL3 mediates α_{2B}-AR interaction with Sec24C/D, the components of ER-derived COPII transport vesicles, and that mutation of this motif reduces the ER export and the cell surface transport of the receptor (23). These data also imply that the cargo α_{2B}-AR may use the same motif to physically associate with distinct transport machineries to direct its export trafficking at different transport steps. It is possible that interaction of the 3R motif with Sec24 modulates the exit from the ER as well as the transport of newly synthesized α_{2B}-AR from the ER to the Golgi body, whereas the 3R motif interaction with GGA3 regulates the post-Golgi export trafficking. In agreement with this possibility, the same di-acidic motif has been demonstrated to interact with Sec24 and AP3 to control vesicular stomatitis virus protein G (VSVG) transport from the ER and the Golgi body, respectively (44, 45). Nevertheless, this study, together with many other reports, indicates that GPCRs may directly interact with the transport machineries to control their export trafficking (23, 24, 46).

Our data presented in this paper clearly reveal a role of GGA3 in the cell surface export of α_{2B}-AR and represent the first demonstration of the functional importance of the GGA family proteins in GPCR trafficking. However, there are many unanswered questions related to the regulation of GPCR transport by GGAs, such as the following. (i) Does GGA3 modulate the cell surface transport of many other GPCRs? (ii) Are other GGA family proteins (i.e., GGA1 and GGA2) involved in the transport of α_{2B}-AR

or other GPCRs? (iii) If so, what molecular mechanisms are used? To address these interesting questions will significantly enhance our understanding of the GGA family protein function in vesicle-mediated GPCR trafficking. As great progress has been achieved over the past several years in defining the roles of transport machinery, regulatory proteins, and trafficking motifs in the cell surface movement of GPCRs *en route* from the ER and the Golgi body (47–56), further elucidation of the export mechanisms of GPCRs may reveal novel therapeutic targets for effective therapy of human diseases, involving abnormal trafficking of GPCRs.

ACKNOWLEDGMENTS

We are grateful to Juan S. Bonifacino, Stuart Kornfeld, and Jeffrey L. Benovic for sharing reagents. We also appreciate the efforts of Jianhui Guo in generating inducible cells expressing HA-α_{2B}-AR in G. Wu's laboratory.

FUNDING INFORMATION

HHS | NIH | National Institute of General Medical Sciences (NIGMS) provided funding to Guangyu Wu under grant number GM076167. HHS | NIH | National Institute of General Medical Sciences (NIGMS) provided funding to Nevin A. Lambert under grant number GM078319. DOD | Congressionally Directed Medical Research Programs (CDMRP) provided funding to Alvin V. Terry, Jr., under grant number W81XWH-12-1-0536. HHS | NIH | National Institute of Environmental Health Sciences (NIEHS) provided funding to Alvin V. Terry, Jr., under grant number ES012241.

The funders had no role in study design, data collection and interpretation, or the decision to submit the work for publication.

REFERENCES

1. **Kobilka BK.** 2011. Structural insights into adrenergic receptor function and pharmacology. Trends Pharmacol Sci **32:**213–218. http://dx.doi.org/10.1016/j.tips.2011.02.005.
2. **Pierce KL, Premont RT, Lefkowitz RJ.** 2002. Seven-transmembrane receptors. Nat Rev Mol Cell Biol **3:**639–650. http://dx.doi.org/10.1038/nrm908.
3. **Conn PM, Ulloa-Aguirre A, Ito J, Janovick JA.** 2007. G protein-coupled receptor trafficking in health and disease: lessons learned to prepare for therapeutic mutant rescue in vivo. Pharmacol Rev **59:**225–250. http://dx.doi.org/10.1124/pr.59.3.2.
4. **Morello JP, Bichet DG.** 2001. Nephrogenic diabetes insipidus. Annu Rev Physiol **63:**607–630. http://dx.doi.org/10.1146/annurev.physiol.63.1.607.
5. **Stojanovic A, Hwa J.** 2002. Rhodopsin and retinitis pigmentosa: shedding light on structure and function. Receptors Channels **8:**33–50. http://dx.doi.org/10.1080/10606820212137.
6. **Hanyaloglu AC, von Zastrow M.** 2008. Regulation of GPCRs by endocytic membrane trafficking and its potential implications. Annu Rev Pharmacol Toxicol **48:**537–568. http://dx.doi.org/10.1146/annurev.pharmtox.48.113006.094830.
7. **Marchese A, Paing MM, Temple BR, Trejo J.** 2008. G protein-coupled receptor sorting to endosomes and lysosomes. Annu Rev Pharmacol Toxicol **48:**601–629. http://dx.doi.org/10.1146/annurev.pharmtox.48.113006.094646.
8. **Boucher R, Larkin H, Brodeur J, Gagnon H, Theriault C, Lavoie C.** 2008. Intracellular trafficking of LRP9 is dependent on two acidic cluster/dileucine motifs. Histochem Cell Biol **130:**315–327. http://dx.doi.org/10.1007/s00418-008-0436-5.
9. **Doray B, Bruns K, Ghosh P, Kornfeld S.** 2002. Interaction of the cation-dependent mannose 6-phosphate receptor with GGA proteins. J Biol Chem **277:**18477–18482. http://dx.doi.org/10.1074/jbc.M201879200.
10. **Doray B, Knisely JM, Wartman L, Bu G, Kornfeld S.** 2008. Identification of acidic dileucine signals in LRP9 that interact with both GGAs and AP-1/AP-2. Traffic **9:**1551–1562. http://dx.doi.org/10.1111/j.1600-0854.2008.00786.x.
11. **Misra S, Puertollano R, Kato Y, Bonifacino JS, Hurley JH.** 2002. Structural basis for acidic-cluster-dileucine sorting-signal recognition by VHS domains. Nature **415:**933–937. http://dx.doi.org/10.1038/415933a.
12. **Nielsen MS, Gustafsen C, Madsen P, Nyengaard JR, Hermey G, Bakke O, Mari M, Schu P, Pohlmann R, Dennes A, Petersen CM.** 2007. Sorting by the cytoplasmic domain of the amyloid precursor protein binding receptor SorLA. Mol Cell Biol **27:**6842–6851. http://dx.doi.org/10.1128/MCB.00815-07.
13. **Nielsen MS, Madsen P, Christensen EI, Nykjaer A, Gliemann J, Kasper D, Pohlmann R, Petersen CM.** 2001. The sortilin cytoplasmic tail conveys Golgi-endosome transport and binds the VHS domain of the GGA2 sorting protein. EMBO J **20:**2180–2190. http://dx.doi.org/10.1093/emboj/20.9.2180.
14. **Puertollano R, Aguilar RC, Gorshkova I, Crouch RJ, Bonifacino JS.** 2001. Sorting of mannose 6-phosphate receptors mediated by the GGAs. Science **292:**1712–1716. http://dx.doi.org/10.1126/science.1060750.
15. **Shiba T, Takatsu H, Nogi T, Matsugaki N, Kawasaki M, Igarashi N, Suzuki M, Kato R, Earnest T, Nakayama K, Wakatsuki S.** 2002. Structural basis for recognition of acidic-cluster dileucine sequence by GGA1. Nature **415:**937–941. http://dx.doi.org/10.1038/415937a.
16. **Takatsu H, Katoh Y, Shiba Y, Nakayama K.** 2001. Golgi-localizing, gamma-adaptin ear homology domain, ADP-ribosylation factor-binding (GGA) proteins interact with acidic dileucine sequences within the cytoplasmic domains of sorting receptors through their Vps27p/Hrs/STAM (VHS) domains. J Biol Chem **276:**28541–28545. http://dx.doi.org/10.1074/jbc.C100218200.
17. **Zhu Y, Doray B, Poussu A, Lehto VP, Kornfeld S.** 2001. Binding of GGA2 to the lysosomal enzyme sorting motif of the mannose 6-phosphate receptor. Science **292:**1716–1718. http://dx.doi.org/10.1126/science.1060896.
18. **Dores MR, Paing MM, Lin H, Montagne WA, Marchese A, Trejo J.** 2012. AP-3 regulates PAR1 ubiquitin-independent MVB/lysosomal sorting via an ALIX-mediated pathway. Mol Biol Cell **23:**3612–3623. http://dx.doi.org/10.1091/mbc.E12-03-0251.
19. **Kim YM, Benovic JL.** 2002. Differential roles of arrestin-2 interaction with clathrin and adaptor protein 2 in G protein-coupled receptor trafficking. J Biol Chem **277:**30760–30768. http://dx.doi.org/10.1074/jbc.M204528200.
20. **Laporte SA, Oakley RH, Zhang J, Holt JA, Ferguson SS, Caron MG, Barak LS.** 1999. The beta2-adrenergic receptor/betaarrestin complex recruits the clathrin adaptor AP-2 during endocytosis. Proc Natl Acad Sci U S A **96:**3712–3717. http://dx.doi.org/10.1073/pnas.96.7.3712.
21. **Hanyaloglu AC, McCullagh E, von Zastrow M.** 2005. Essential role of Hrs in a recycling mechanism mediating functional resensitization of cell signaling. EMBO J **24:**2265–2283. http://dx.doi.org/10.1038/sj.emboj.7600688.
22. **Hanyaloglu AC, von Zastrow M.** 2007. A novel sorting sequence in the beta2-adrenergic receptor switches recycling from default to the Hrs-dependent mechanism. J Biol Chem **282:**3095–3104. http://dx.doi.org/10.1074/jbc.M605398200.
23. **Dong C, Nichols CD, Guo J, Huang W, Lambert NA, Wu G.** 2012. A triple arg motif mediates alpha(2B)-adrenergic receptor interaction with Sec24C/D and export. Traffic **13:**857–868. http://dx.doi.org/10.1111/j.1600-0854.2012.01351.x.
24. **Li C, Fan Y, Lan TH, Lambert NA, Wu G.** 2012. Rab26 modulates the cell surface transport of alpha2-adrenergic receptors from the Golgi. J Biol Chem **287:**42784–42794. http://dx.doi.org/10.1074/jbc.M112.410936.
25. **Dell'Angelica EC, Puertollano R, Mullins C, Aguilar RC, Vargas JD, Hartnell LM, Bonifacino JS.** 2000. GGAs: a family of ADP ribosylation factor-binding proteins related to adaptors and associated with the Golgi complex. J Cell Biol **149:**81–94. http://dx.doi.org/10.1083/jcb.149.1.81.
26. **Dong C, Li C, Wu G.** 2011. Regulation of alpha(2B)-adrenergic receptor-mediated extracellular signal-regulated kinase 1/2 (ERK1/2) activation by ADP-ribosylation factor 1. J Biol Chem **286:**43361–43369. http://dx.doi.org/10.1074/jbc.M111.267286.
27. **Fan Y, Li C, Guo J, Hu G, Wu G.** 2012. A single lys residue on the first intracellular loop modulates the endoplasmic reticulum export and cell-surface expression of alpha2A-adrenergic receptor. PLoS One **7:**e50416. http://dx.doi.org/10.1371/journal.pone.0050416.
28. **Wu G, Zhao G, He Y.** 2003. Distinct pathways for the trafficking of angiotensin II and adrenergic receptors from the endoplasmic reticulum to the cell surface: Rab1-independent transport of a G protein-coupled receptor. J Biol Chem **278:**47062–47069. http://dx.doi.org/10.1074/jbc.M305707200.

29. **Ghosh P, Griffith J, Geuze HJ, Kornfeld S.** 2003. Mammalian GGAs act together to sort mannose 6-phosphate receptors. J Cell Biol **163:**755–766. http://dx.doi.org/10.1083/jcb.200308038.
30. **Hirst J, Sahlender DA, Choma M, Sinka R, Harbour ME, Parkinson M, Robinson MS.** 2009. Spatial and functional relationship of GGAs and AP-1 in Drosophila and HeLa cells. Traffic **10:**1696–1710. http://dx.doi.org/10.1111/j.1600-0854.2009.00983.x.
31. **Duvernay MT, Zhou F, Wu G.** 2004. A conserved motif for the transport of G protein-coupled receptors from the endoplasmic reticulum to the cell surface. J Biol Chem **279:**30741–30750. http://dx.doi.org/10.1074/jbc.M313881200.
32. **Duvernay MT, Dong C, Zhang X, Robitaille M, Hebert TE, Wu G.** 2009. A single conserved leucine residue on the first intracellular loop regulates ER export of G protein-coupled receptors. Traffic **10:**552–566. http://dx.doi.org/10.1111/j.1600-0854.2009.00890.x.
33. **Dong C, Yang L, Zhang X, Gu H, Lam ML, Claycomb WC, Xia H, Wu G.** 2010. Rab8 interacts with distinct motifs in alpha2B- and beta2-adrenergic receptors and differentially modulates their transport. J Biol Chem **285:**20369–20380. http://dx.doi.org/10.1074/jbc.M109.081521.
34. **DeGraff JL, Gagnon AW, Benovic JL, Orsini MJ.** 1999. Role of arrestins in endocytosis and signaling of alpha2-adrenergic receptor subtypes. J Biol Chem **274:**11253–11259. http://dx.doi.org/10.1074/jbc.274.16.11253.
35. **Vazquez SM, Mladovan AG, Perez C, Bruzzone A, Baldi A, Luthy IA.** 2006. Human breast cell lines exhibit functional alpha2-adrenoceptors. Cancer Chemother Pharmacol **58:**50–61. http://dx.doi.org/10.1007/s00280-005-0130-4.
36. **Bylund DB, Ray-Prenger C.** 1989. Alpha-2A and alpha-2B adrenergic receptor subtypes: attenuation of cyclic AMP production in cell lines containing only one receptor subtype. J Pharmacol Exp Ther **251:**640–644.
37. **Li C, Horn JP.** 2008. Differential Inhibition of Ca2+ channels by alpha2-adrenoceptors in three functional subclasses of rat sympathetic neurons. J Neurophysiol **100:**3055–3063. http://dx.doi.org/10.1152/jn.90590.2008.
38. **Li YW, Guyenet PG, Bayliss DA.** 1998. Voltage-dependent calcium currents in bulbospinal neurons of neonatal rat rostral ventrolateral medulla: modulation by alpha2-adrenergic receptors. J Neurophysiol **79:**583–594.
39. **Timmons SD, Geisert E, Stewart AE, Lorenzon NM, Foehring RC.** 2004. alpha2-Adrenergic receptor-mediated modulation of calcium current in neocortical pyramidal neurons. Brain Res **1014:**184–196. http://dx.doi.org/10.1016/j.brainres.2004.04.025.
40. **Dong C, Zhang X, Zhou F, Dou H, Duvernay MT, Zhang P, Wu G.** 2010. ADP-ribosylation factors modulate the cell surface transport of G protein-coupled receptors. J Pharmacol Exp Ther **333:**174–183. http://dx.doi.org/10.1124/jpet.109.161489.
41. **Binda C, Genier S, Cartier A, Larrivee JF, Stankova J, Young JC, Parent JL.** 2014. A G protein-coupled receptor and the intracellular synthase of its agonist functionally cooperate. J Cell Biol **204:**377–393. http://dx.doi.org/10.1083/jcb.201304015.
42. **Gimelbrant AA, Haley SL, McClintock TS.** 2001. Olfactory receptor trafficking involves conserved regulatory steps. J Biol Chem **276:**7285–7290. http://dx.doi.org/10.1074/jbc.M005433200.
43. **Jacobsen L, Madsen P, Nielsen MS, Geraerts WP, Gliemann J, Smit AB, Petersen CM.** 2002. The sorLA cytoplasmic domain interacts with GGA1 and -2 and defines minimum requirements for GGA binding. FEBS Lett **511:**155–158. http://dx.doi.org/10.1016/S0014-5793(01)03299-9.
44. **Nishimura N, Balch WE.** 1997. A di-acidic signal required for selective export from the endoplasmic reticulum. Science **277:**556–558. http://dx.doi.org/10.1126/science.277.5325.556.
45. **Nishimura N, Plutner H, Hahn K, Balch WE.** 2002. The delta subunit of AP-3 is required for efficient transport of VSV-G from the trans-Golgi network to the cell surface. Proc Natl Acad Sci U S A **99:**6755–6760. http://dx.doi.org/10.1073/pnas.092150699.
46. **Wang G, Wu G.** 2012. Small GTPase regulation of GPCR anterograde trafficking. Trends Pharmacol Sci **33:**28–34. http://dx.doi.org/10.1016/j.tips.2011.09.002.
47. **Achour L, Labbe-Jullie C, Scott MG, Marullo S.** 2008. An escort for GPCRs: implications for regulation of receptor density at the cell surface. Trends Pharmacol Sci **29:**528–535. http://dx.doi.org/10.1016/j.tips.2008.07.009.
48. **Bermak JC, Li M, Bullock C, Zhou QY.** 2001. Regulation of transport of the dopamine D1 receptor by a new membrane-associated ER protein. Nat Cell Biol **3:**492–498. http://dx.doi.org/10.1038/35074561.
49. **Carrel D, Hamon M, Darmon M.** 2006. Role of the C-terminal di-leucine motif of 5-HT1A and 5-HT1B serotonin receptors in plasma membrane targeting. J Cell Sci **119:**4276–4284. http://dx.doi.org/10.1242/jcs.03189.
50. **Dong C, Filipeanu CM, Duvernay MT, Wu G.** 2007. Regulation of G protein-coupled receptor export trafficking. Biochim Biophys Acta **1768:**853–870. http://dx.doi.org/10.1016/j.bbamem.2006.09.008.
51. **Donnellan PD, Kimbembe CC, Reid HM, Kinsella BT.** 2011. Identification of a novel endoplasmic reticulum export motif within the eighth alpha-helical domain (alpha-H8) of the human prostacyclin receptor. Biochim Biophys Acta **1808:**1202–1218. http://dx.doi.org/10.1016/j.bbamem.2011.01.003.
52. **Guo Y, Jose PA.** 2011. C-terminal di-leucine motif of dopamine D(1) receptor plays an important role in its plasma membrane trafficking. PLoS One **6:**e29204. http://dx.doi.org/10.1371/journal.pone.0029204.
53. **Lodowski KH, Lee R, Ropelewski P, Nemet I, Tian G, Imanishi Y.** 2013. Signals governing the trafficking and mistrafficking of a ciliary GPCR, rhodopsin. J Neurosci **33:**13621–13638. http://dx.doi.org/10.1523/JNEUROSCI.1520-13.2013.
54. **Sawyer GW, Ehlert FJ, Shults CA.** 2010. A conserved motif in the membrane proximal C-terminal tail of human muscarinic m1 acetylcholine receptors affects plasma membrane expression. J Pharmacol Exp Ther **332:**76–86. http://dx.doi.org/10.1124/jpet.109.160986.
55. **Schulein R, Hermosilla R, Oksche A, Dehe M, Wiesner B, Krause G, Rosenthal W.** 1998. A dileucine sequence and an upstream glutamate residue in the intracellular carboxyl terminus of the vasopressin V2 receptor are essential for cell surface transport in COS.M6 cells. Mol Pharmacol **54:**525–535.
56. **Zhang X, Dong C, Wu Q J, Balch WE, Wu G.** 2011. Di-acidic motifs in the membrane-distal C termini modulate the transport of angiotensin II receptors from the endoplasmic reticulum to the cell surface. J Biol Chem **286:**20525–20535. http://dx.doi.org/10.1074/jbc.M111.222034.